

Essential role for Atox1 in the copper-mediated intracellular trafficking of the Menkes ATPase

Iqbal Hamza*, Joseph Prohaska†, and Jonathan D. Gitlin**

*Edward Mallinckrodt Department of Pediatrics, Washington University School of Medicine, St. Louis, MO 63110; and †Department of Biochemistry and Molecular Biology, University of Minnesota School of Medicine, Duluth, MN 55812

Edited by Richard D. Palmiter, University of Washington School of Medicine, Seattle, WA, and approved December 9, 2002 (received for review October 14, 2002)

The metallochaperone Atox1 directly interacts with the copper-transporting ATPases and plays a critical role in perinatal copper homeostasis. To determine the cell biological mechanisms of Atox1 function, intracellular copper metabolism, and Menkes ATPase abundance, localization and trafficking were examined in immortalized fibroblast cell lines derived from *Atox1*^{+/+} and *Atox1*^{-/-} embryos. Consistent with the proposed role for Atox1 in copper delivery to the secretory pathway, a marked increase in intracellular copper content secondary to impaired copper efflux was observed in *Atox1*-deficient cells. Although the localization of the Menkes ATPase was identical in *Atox1*^{+/+} and *Atox1*^{-/-} cells under conditions of equivalent intracellular copper content, a significant impairment in copper-mediated Menkes ATPase trafficking was observed in the absence of Atox1. When quantitative confocal immunofluorescence was used, significant differences in the time and dose-dependent trafficking of the Menkes ATPase from the Golgi compartment in response to copper were observed between *Atox1*^{+/+} and *Atox1*^{-/-} cells. These data reveal an essential role for Atox1 in establishing the threshold for copper-dependent movement of the copper-transporting ATPases within the secretory compartment and that, in the absence of Atox1, this movement alone is not sufficient to restore normal copper efflux. Taken together, these findings provide a cell biological model for the role of this metallochaperone under the physiological conditions of copper limitation in mammalian cells.

Copper is an essential micronutrient and plays a critical biochemical role in diverse metabolic pathways in all aerobic organisms (1). The essential need for copper as well as the toxicity of this metal is dramatically underscored by the two inherited disorders of copper metabolism, Menkes disease and Wilson disease (2). Despite the strikingly different clinical phenotypes, these disorders result from loss-of-function mutations in genes encoding homologous copper-transporting P-type ATPases. These ATPases reside in the secretory pathway and transport copper into this compartment for subsequent incorporation into nascent cuproproteins and efflux from the cell (2, 3). An increase in the intracellular copper concentration results in the trafficking of these ATPases from the Golgi to a cytoplasmic, vesicular compartment (4, 5). This process provides a rapid, posttranslational mechanism for the immediate response of the cell to changes in copper content that is critical for maintaining intracellular copper homeostasis (6).

Recent studies in yeast have revealed that under physiological circumstances intracellular copper availability is extraordinarily restricted (7). As a result, the delivery of copper to specific pathways within the cell is mediated by a family of proteins termed metallochaperones that function to provide copper directly to target pathways while protecting this metal from intracellular scavenging (8–10). The metallochaperone Atox1 interacts directly with the Menkes and Wilson ATPases, delivering copper to these proteins in the secretory pathway (11–13). Genetic studies with *Atox1*^{-/-} mice reveal that this metallochaperone plays a critical role in perinatal copper homeostasis, indicating a physiological role for Atox1 in mammalian copper

metabolism (14). Despite these biochemical and genetic findings, the precise cell biological mechanisms of Atox1 function in intracellular copper homeostasis remain unknown. In this study, a cellular model of Atox1 deficiency was developed and used to elucidate the cell biological mechanisms of Atox1 function.

Materials and Methods

Cell Culture and Antibodies. Cell lines were routinely cultured in basal growth media composed of DMEM (GIBCO/BRL) with 10% bovine serum supplemented with penicillin/streptomycin/glutamine. Copper content in this batch of basal media was determined to be 252 nM by atomic absorption spectroscopy. Low-serum media contain identical components with 1% bovine serum. For cell culture experiments, *Atox1*^{+/+} and *Atox1*^{-/-} mouse embryonic fibroblasts from embryonic day 12.5 embryos were isolated and cultured in basal media (15). After the first passage these mouse embryonic fibroblasts were genotyped by PCR analysis as described (14). The *mottled* mouse (*Mo*^{br-J}) fibroblast cell line 802-1^{Mnk} (*Mo*^{-Y}, *Mt*^{-/+}) and the corresponding wild-type cell line 802-5 (*Mo*^{+Y}, *Mt*^{-/+}) were cultured as described (16). For copper dose-response experiments, an identical number of *Atox1*^{+/+} and *Atox1*^{-/-} cells were allowed to adhere onto tissue culture plates in basal medium. After 18 h, cells were incubated in the presence of 200 μM bathocuproine disulfonic acid (BCS) in low-serum media. For copper treatment the BCS containing media was aspirated off at various time intervals and cells were washed twice with PBS followed by addition of copper in low-serum media. BCS (20 mM) and copper chloride (10 mM) stocks were prepared fresh in tissue culture grade water and filter sterilized before use.

Rabbit polyclonal antibody to SOD1 (Stressgen Biotechnologies, Victoria, Canada), mouse monoclonal antibodies to simian virus 40 (SV40) T antigen (Pab101):sc147 (Santa Cruz Biotechnology) and GS28 (Golgi Sampler kit; BD Biosciences) were used according to the manufacturer's recommendations. Rabbit polyclonal antisera to Atox1 was used as described (11). To generate Menkes antibody, a 21-aa peptide, SEPDKHSLLYGDFREDDTTL, corresponding to the C-terminal end of the Menkes protein was synthesized and used to produce polyclonal antisera in rabbits (Covance Research Products, Denver, PA). Experiments were performed with antisera that was affinity purified against the Menkes peptide coupled to cyanogen bromide-activated Sepharose 4B column.

Cell immortalization and immunoblotting. Retroviral infections were performed on primary *Atox1*^{+/+} and *Atox1*^{-/-} mouse embryo fibroblasts by using conditioned media from Ψ2U195 cell line producing SV40 large T antigen as described (17). Cells were serially diluted 48 h after infection into media containing G418 (250 μg/ml) and allowed to form single clones. Multiple G418-resistant clones were picked and grown for at least five

This paper was submitted directly (Track II) to the PNAS office.

Abbreviations: BCS, bathocuproine disulfonic acid; SV40, simian virus 40.

*To whom correspondence should be addressed. E-mail: gitlin@kids.wustl.edu.

additional passages, and from these, three individual clones were expanded for further analysis. Cells lysates were prepared in 50 mM Hepes, pH 7.4/0.1% Nonidet P-40/150 mM NaCl supplemented with protease inhibitor mixture (Calbiochem) on ice for 15 min, followed by centrifugation for 10 min at $6,000 \times g$ at 4°C . Protein concentration for all samples was determined by Bradford's method (Bio-Rad). For immunoblotting, lysates were heated at 100°C for 10 min in the presence of SDS sample buffer containing 2-mercaptoethanol and centrifuged for 5 min at $16,000 \times g$ at 4°C before loading the supernatant onto SDS/PAGE. For analysis of Menkes protein, cell lysates were processed as above without heating. Proteins were separated by SDS/PAGE, transferred to nitrocellulose, and detected by either the SuperSignal West Pico or West Femto Chemiluminescence kits (Pierce) using goat anti-rabbit and anti-mouse horseradish peroxidase-conjugated secondary antibody (Pierce)

Immunofluorescence Microscopy and Image Quantification. For immunostaining, cells grown on glass coverslips were fixed in fresh 4% paraformaldehyde and permeabilized in 0.2% Triton X-100 as described (5). In some experiments, cells were incubated in 200 μM BCS for 48 h followed by CuCl_2 treatment. Nonspecific signals were blocked with SuperBlock Blocking Buffer (Pierce) in PBS for 1 h followed by incubations in the same blocking media containing Menkes (1:8,000) and GS28 (1:3,000) primary antibodies and goat anti-rabbit and anti-mouse secondary antibodies conjugated to Alexa 546 and Alexa 488 (Molecular Probes) fluorophores. Coverslips were mounted by using ProLong Antifade (Molecular Probes) and analyzed by using an epifluorescence microscope (BX60, Olympus, New Hyde Park, NY). For confocal microscopy studies, a laser-scanning microscope (BX61WI FV500, Olympus), equipped with Argon 488, Krypton 568, and HeNe 633 lasers and fitted with a PlanApo $\times 60$ oil immersion objective, was used. For multichannel imaging, fluorescent dyes were imaged sequentially to eliminate cross-talk between the channels, and serial Z stacks of images were acquired by using a pinhole aperture of 200 μm . Serial and individual sections were analyzed for fluorescent signal overlap first by visual inspection, and then quantitated by using the FLUOVIEW FV500 Version 3.3 program (Olympus). The GS28 signal was used as the reference channel, and all fluorescent structures representing the Golgi were outlined with a region of interest (ROI). This ROI was then projected onto the underlying Menkes signal in the 568 channel, and the fluorescent intensity corresponding to the Menkes protein evaluated. Analyses were done with multiple ROI in series, and plotted as integrated intensity versus Z axis (μm). The values obtained by these analyses were imported into a statistical program, and each data point was calculated as the percentage ratio of the signal intensity in the experimental sample (copper treated) to the signal intensity in the control sample (BCS treated). About seven separate scans were performed on every coverslip, and each scan comprised an average of 15–18 cells and five Z-stack sections. Thus, at least 105 cells were sampled per data point and each experiment was repeated at least four times. Statistical analysis for P values were calculated by using a one-way ANOVA with a Student–Newman–Keuls multiple comparison test using GRAPHPAD INSTANT Version 3.01.

Metabolic Labeling and Copper Measurements. For copper retention studies, 2×10^5 cells were allowed to adhere onto 35-mm petri dishes before incubation for 68 h with 8×10^6 cpm of ^{64}Cu in basal culture medium (14). The cells were then washed three times with ice-cold PBS, lysed with PBS containing 1% SDS, and analyzed for ^{64}Cu retention by using a Packard Gamma Counter. For copper uptake, cells were incubated for 6 and 10 min time points in the presence of 0.5, 10, and 100 μM ^{64}Cu at 37°C . The experiment was done in parallel at 4°C for background correc-

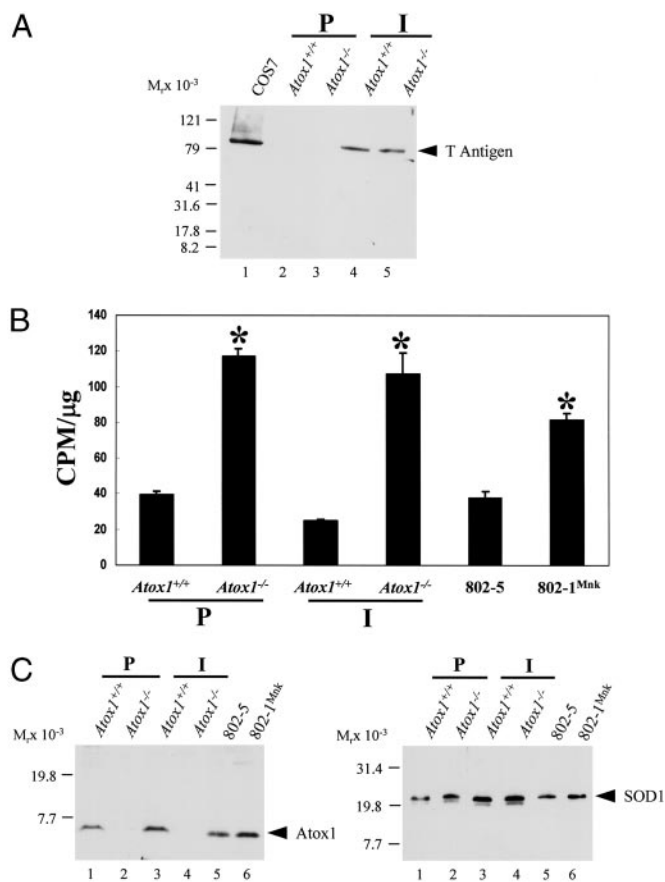


Fig. 1. Characterization of Atox1-deficient cells. (A) Immunoblot analysis of SV40 large T antigen in primary (P) and immortalized (I) embryonic fibroblasts. Cell lysate (100 μg) was separated by 4–20% SDS/PAGE and analyzed with SV40 T antigen antisera followed by chemiluminescent detection. Cos7 cells express T antigen and were used as a positive control. (B) Copper retention was determined in cultured Atox1^{+/+} and Atox1^{-/-} cells, and cell lines were derived from *Mo^{br-J}* mice (802-1Mnk) or the corresponding wild-type control (802-5). A total of 2×10^5 cells were incubated with 8×10^6 cpm of ^{64}Cu . After 68 h, the cells were washed, lysed, and analyzed for ^{64}Cu retained by using a γ counter. Each data point represents the mean \pm SEM from three separate experiments performed in triplicate and expressed as cpm/ μg of total cell protein (*, $P < 0.05$). (C) Immunoblot analysis of Atox1 protein in mouse fibroblasts. Cell lysate (100 μg) was separated by 10–20% Tricine SDS/PAGE and probed with Atox1 antisera followed by chemiluminescent detection. This immunoblot was stripped to remove Atox1 antibodies and reprobed with SOD1 antisera (D). SOD1 migrates slower than the expected 16 kDa on Tricine SDS/PAGE used to analyze low molecular weight proteins such as Atox1.

tion. Counts (cpm) obtained were normalized to total protein concentration, as determined by the bicinchoninic acid method (Sigma). To measure total steady state copper content, 90% confluent Atox1^{+/+} and Atox1^{-/-} cultured cells were wet digested with nitric acid and analyzed by graphite furnace atomic absorption spectroscopy (18).

Results

To create a stable cell line deficient in Atox1, fibroblasts were cultured from Atox1^{+/+} and Atox1^{-/-} embryonic day-12.5 embryos and transduced with a retrovirus expressing SV40 T antigen. Immunoblot analysis of lysates from late passage cells revealed the presence of a 94-kDa large T antigen, confirming the process of immortalization (Fig. 1A). To examine copper homeostasis in these immortalized cells, copper accumulation and efflux were examined after metabolic labeling with ^{64}Cu . These studies revealed that, consistent with previous observa-

tions in primary *Atox1*^{-/-} and Menkes-deficient 802-1 cells (14), immortalized *Atox1*^{-/-} cells accumulated significantly greater amounts of copper when compared with wild-type cells (Fig. 1B) and that this defect was the direct result of impaired copper efflux (data not shown). Immunoblot analysis of these cell lysates revealed equivalent amounts of Atox1 in *Atox1*^{+/+}, 802-5^{Mnk}, and 802-1 cell lines, indicating that the observed changes in cellular copper content in these cells did not affect the steady state levels of this protein (Fig. 1C). Furthermore, the abundance (Fig. 1D) and activity (data not shown) of Cu/Zn superoxide dismutase, a cytosolic cuproprotein, was equivalent in each of these cell lines, indicating that the absence of Atox1 and the resultant increased intracellular copper content in the immortalized cell line did not effect other copper chaperone-dependent pathways.

The above data indicate that the *Atox1*^{-/-} immortalized cell line is an appropriate model for analysis of the role of Atox1 in copper trafficking to the secretory pathway of the cell. Previous studies have demonstrated that the Menkes copper-transporting ATPase is essential for cellular copper efflux and homeostasis in mouse embryonic fibroblasts (16). Therefore, as Atox1 directly interacts with the Menkes ATPase (11, 12), we hypothesized that the impaired copper efflux and resultant copper accumulation in *Atox1*^{-/-} cells might result from alterations in either the abundance, localization, or trafficking of this ATPase. Immunoblot analysis of cell lysates from *Atox1*^{+/+} and *Atox1*^{-/-} fibroblasts revealed equivalent amounts of the Menkes ATPase in primary cell lines (Fig. 2A). A 2-fold increase in the abundance of the Menkes ATPase was consistently observed in immortalized *Atox1*^{-/-} cells compared with the wild-type (Fig. 2A, lanes 3 and 4). However, this difference was without effect on copper homeostasis in these cells, as copper retention (Figs. 1B and 2A) and efflux (data not shown) was equivalent to that observed in the primary *Atox1*^{-/-} cells. As observed previously, the 802-1 cell line derived from the *mottled* mouse contained significantly less Menkes ATPase compared with the 802-5 cells derived from littermate controls (Fig. 2A, lanes 5 and 6). To precisely determine the intracellular localization of the Menkes ATPase in mouse embryonic fibroblasts, Menkes sufficient 802-5 cells were cultured in growth media and processed for immunofluorescence by using antisera specific for either the murine Menkes ATPase or a series of proteins known to localize to specific compartments within the secretory pathway (data not shown). This detailed analysis revealed expression of the Menkes ATPase in a perinuclear compartment directly overlapping with the expression of GS28, a 28-kDa SNARE protein that mediates vesicular transport and trafficking within the Golgi compartments (19) (Fig. 2B Upper). The specificity of this murine Menkes ATPase antisera was confirmed by a significant decrease in this signal in Menkes-deficient 802-1 cells (Fig. 2B Lower) despite normal integrity of the Golgi, as revealed by GS28 staining (Fig. 2B Lower).

Similar immunofluorescence studies were next performed in immortalized *Atox1*^{+/+} and *Atox1*^{-/-} cells. As was observed above, the Menkes ATPase localized predominantly to the perinuclear region in *Atox1*^{+/+} cells, overlapping with the expression of GS28 (Fig. 2C). In contrast, identical experiments in *Atox1*^{-/-} cells revealed a striking difference, with the Menkes ATPase present not only in the GS28 compartment but also in a diffuse vesicular compartment throughout the cytoplasm (Fig. 2C). Because our previous data revealed that *Atox1*^{-/-} immortalized cells accumulate copper when cultured in growth medium (Fig. 1B), these distinct differences in the localization of the Menkes ATPase might result from either a direct effect of Atox1 deficiency on Menkes trafficking or a consequence of the increased intracellular copper in these cells. To distinguish between these possibilities, *Atox1*^{+/+} and *Atox1*^{-/-} cells were grown in 200 μM BCS for 48 h to reduce the intracellular copper content to equivalent levels (Table 1). Under these circum-

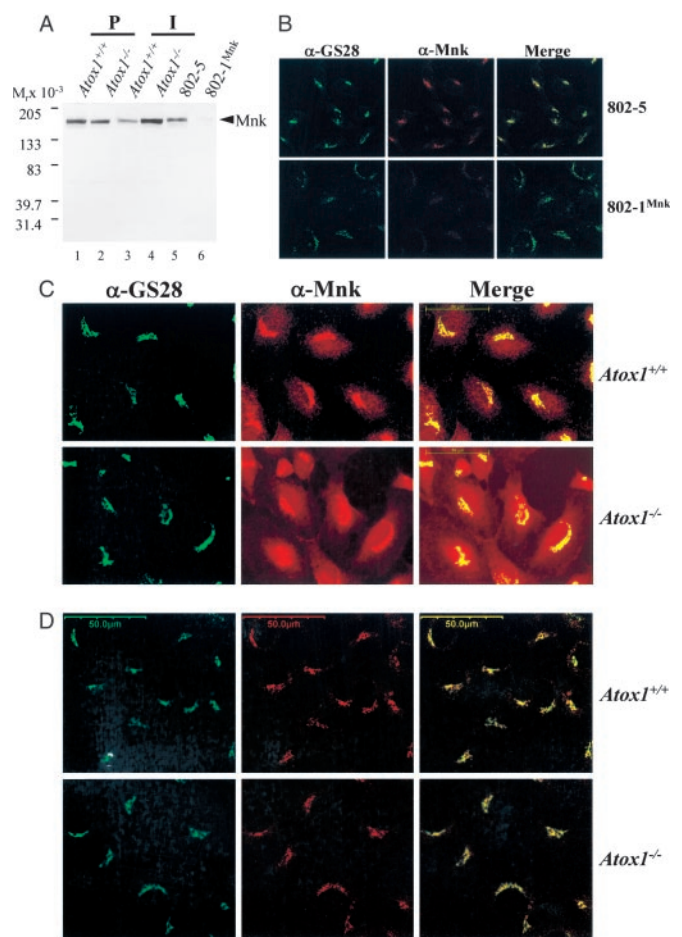


Fig. 2. Immunolocalization of Menkes ATPase in *Atox1*-deficient cells. (A) Immunoblot analysis of Menkes protein in mouse fibroblasts. Cell lysate (100 μg) was separated by 4–20% SDS/PAGE and probed with Menkes antisera (1:2,000) generated against the C terminus of the Menkes ATPase, followed by chemiluminescent detection. Less than 2% of Menkes protein was detected in 802-1 cells compared with wild-type 802-5 cells. (B) Double label indirect immunofluorescence localization (×63) in 802-5 and 802-1 cells grown in basal media, fixed, and stained with GS28 (α-GS28, Alexa 488) and Menkes (α-Mnk, Alexa 546) antibodies, and analyzed by using epifluorescence microscopy. Images of Menkes and GS28 Golgi marker are merged to depict overlapping regions. (Scale bar, 50 μm.) (C and D) Immortalized *Atox1*^{+/+} and *Atox1*^{-/-} cell lines were grown in basal media (C) or in the presence of 200 μM BCS (D) and processed for indirect immunofluorescence studies as described above by using epifluorescence microscopy. (Scale bar, 50 μm.)

stances, an identical intracellular localization of the Menkes ATPase was observed in both cell lines (Fig. 2D), revealing that the cytoplasmic localization of the Menkes ATPase observed in *Atox1*^{-/-} cells (Fig. 2C) was the result of the increased intracellular copper content in *Atox1*^{-/-} cells (Table 1). These distinct differences in the localization of the Menkes ATPase were not the result of immortalization of these cells as similar observations were made with the parental primary cell lines (data not shown).

Taken together, these data reveal that the impaired copper efflux observed in the *Atox1*-deficient cells is not the result of alterations in abundance or localization of Menkes ATPase. However, the differences in the localization of the Menkes ATPase observed in *Atox1*^{+/+} and *Atox1*^{-/-} cells under steady-state conditions (Fig. 2C) suggests the possibility of a critical role for Atox1 in determining the threshold for copper-dependent trafficking of this ATPase. To directly examine this possibility,

Table 1. Copper concentration in *Atox1*^{+/+} and *Atox1*^{-/-} cells by atomic absorption spectroscopy

Growth conditions	Copper, ng/mg	
	<i>Atox1</i> ^{+/+}	<i>Atox1</i> ^{-/-}
Basal media (10% serum)	6.2 ± 1.8	20.2 ± 2*
Low serum media (1% serum)	6.7 ± 0.5	18.2 ± 2.5*
200 μM BCS [†]	4.4 ± 0.4	3.9 ± 0.5
0.5 μM Cu [†]	12.9 ± 1.4	18.4 ± 1.8 ^{NS}
10 μM Cu [†]	21.9 ± 5.5	28.6 ± 7.2 ^{NS}
100 μM Cu [†]	21.3 ± 7.9	17.3 ± 4.1 ^{NS}

Values (triplicates), [Copper] ng/ml total protein are given as mean ± SEM. NS, not significant between *Atox1*^{+/+} and *Atox1*^{-/-} cells and within *Atox1*^{-/-} samples.

**P* < 0.05 between *Atox1*^{+/+} and *Atox1*^{-/-} cells.

[†]Cells were grown in low-serum media with 200 μM BCS for 48 h prior to copper treatment for 3 h.

Atox1^{+/+} and *Atox1*^{-/-} cells were incubated in BCS for 48 h followed by incubation in media with increasing copper concentrations and subsequent immunofluorescent localization of the Menkes ATPase. These studies revealed dose-dependent copper-mediated trafficking of the Menkes ATPase in *Atox1*^{+/+} cells, from the perinuclear Golgi compartment to the cytoplasm (Fig. 3*A Upper*), as has been previously demonstrated for other cell lines (4). In contrast, when these same studies were performed in *Atox1*^{-/-} cells, a marked abrogation of this copper-dependent ATPase trafficking was observed (Fig. 3*A Lower*). These differences in Menkes ATPase trafficking in *Atox1*^{+/+} and *Atox1*^{-/-} cells were not the result of changes in intracellular copper content, as metabolic experiments with ⁶⁴Cu revealed equivalent rates of copper uptake (data not shown) and atomic absorption spectroscopy revealed equivalent amounts of copper in both cell lines at each experimental copper concentration (Table 1).

To more precisely quantitate the effect of *Atox1* deficiency on copper-mediated trafficking of the Menkes ATPase, double-label immunofluorescence was performed by using quantitative confocal microscopy. For these studies, the percentage of Menkes ATPase trafficking out of the Golgi compartment was quantitated as the integrated fluorescence intensity of the Menkes signal highlighted by GS28 versus that appearing in the cytoplasm. When this trafficking was examined in *Atox1*^{+/+} cells, a dose-dependent response was observed between 0.5 and 100 μM copper (Fig. 3*B*). A further increase in the copper content of the growth media did not result in a concomitant increase in Menkes ATPase trafficking from the Golgi, and concentrations greater than 600 μM CuCl₂ resulted in decreased cell viability (data not shown).

This quantitative immunofluorescence assay was next used in *Atox1*^{+/+} and *Atox1*^{-/-} cells to examine the role of *Atox1* in copper-mediated Menkes ATPase trafficking as a function of both time and copper concentration. As shown in Fig. 4*A*, the percentage movement of Menkes protein out of the Golgi in *Atox1*^{+/+} cells was linear for ≈1.5 h at 0.5 μM copper and was saturable with increasing time and copper content. In marked contrast to this observation, *Atox1*^{-/-} cells demonstrated a significant impairment in the copper-mediated movement of the Menkes ATPase out of the Golgi under these same conditions (Fig. 4*A*). When these experiments were repeated at copper concentrations of 10 μM, similar observations were made where again the absence of *Atox1* was associated with a diminution of copper-dependent Menkes ATPase trafficking from the Golgi compartment (Fig. 4*B*). In distinction to these findings, under conditions of 100 μM copper, an equivalent movement of the Menkes ATPase out of the Golgi was observed in the absence

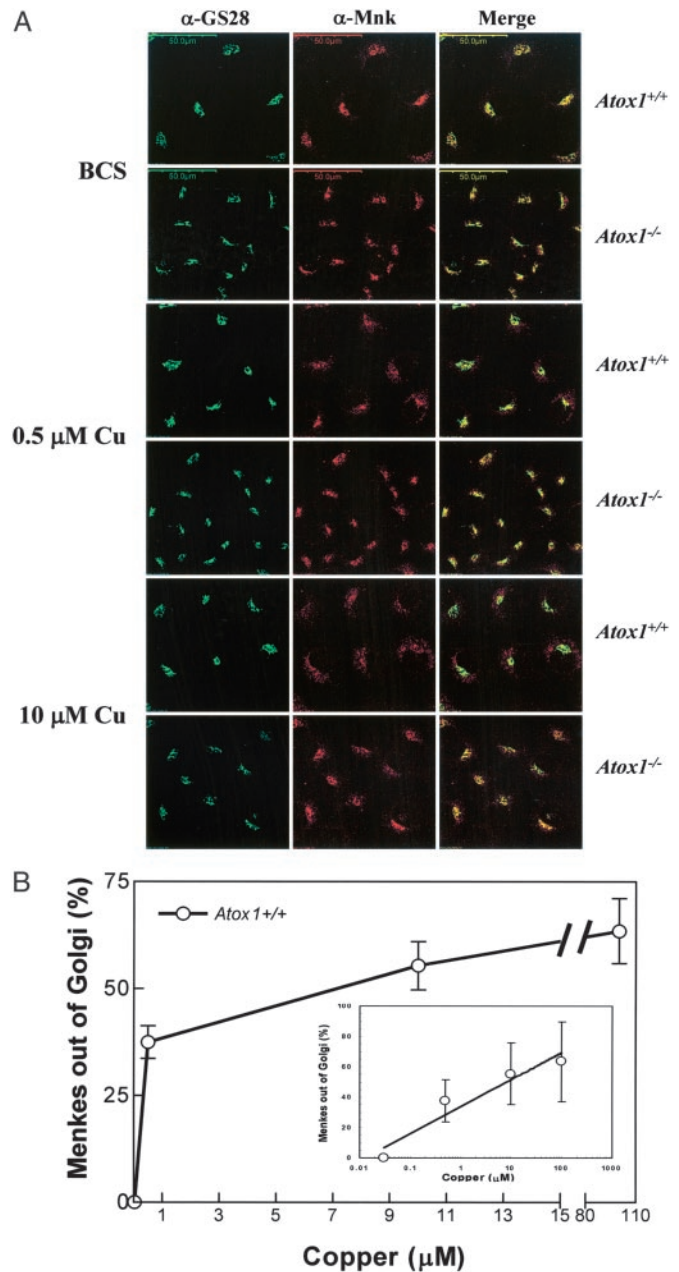


Fig. 3. Characterization of copper-mediated trafficking of Menkes protein. (A) Immortalized *Atox1*^{+/+} and *Atox1*^{-/-} cells were grown on coverslips in the presence of 200 μM BCS for 48 h, followed by the addition of 0.5 or 10 μM CuCl₂ for 1 h to the culture media, and processed for double-label immunofluorescence by using Menkes and GS28 antibodies for analysis with confocal microscopy. Images of Menkes and GS28 are merged to depict overlapping regions. (Scale bar, 50 μm.) (B) Quantitative analysis of Menkes signal in the Golgi was measured in immortalized *Atox1*^{+/+} cells by using double-label immunofluorescence studies as described in *Materials and Methods*. Cells were grown in the presence of 200 μM BCS followed by copper treatment for 3 h, and processed for immunostaining. Overlapping signal intensities were analyzed and quantitated by using a laser scanning confocal Olympus microscope and FLUOVIEW FV500 Version 3.3 program. Each data point represents the mean ± SEM from four separate experiments with a minimum of seven scans per experiment per data point. Each scan is comprised of 15–18 cells or at least 105 cells. (Inset) The same analysis plotted onto a logarithmic x axis (μM) for clarity.

and presence of *Atox1* (Figs. 4*C*). The observation that even under the maximum conditions of stimulation a portion of the Menkes ATPase is detected in the Golgi compartment is con-

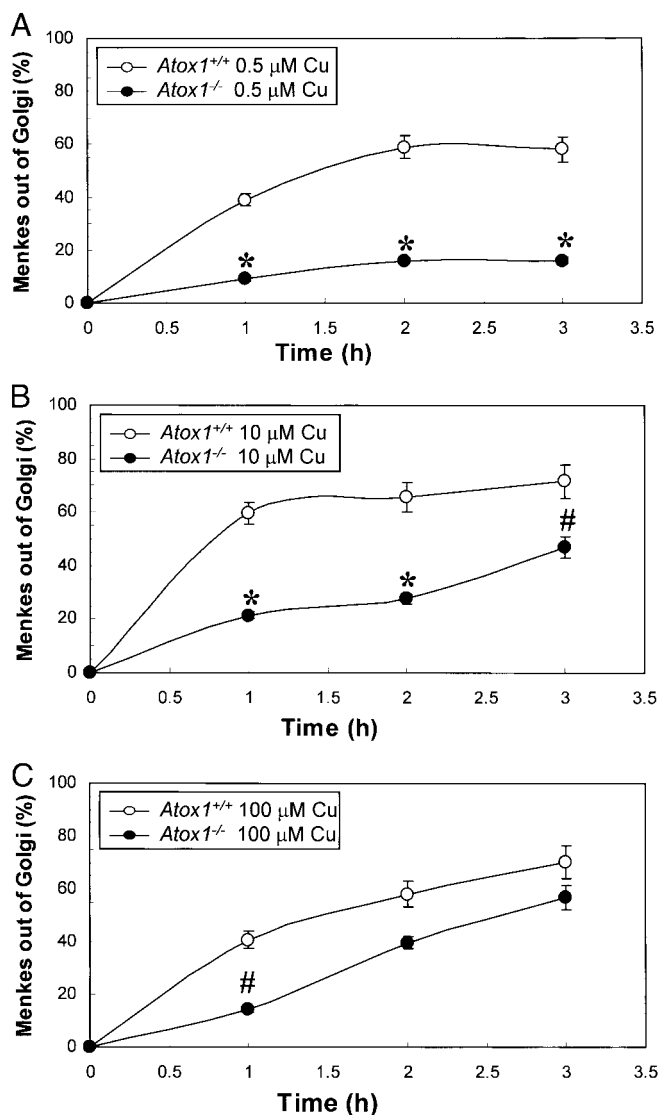


Fig. 4. Time- and dose-dependent trafficking of the Menkes protein. Quantitative immunofluorescence analysis of Menkes signal in the Golgi was measured in immortalized *Atox1*^{+/+} and *Atox1*^{-/-} cells in 200 μ M BCS for 48 h, followed by 1-, 2-, and 3-h incubations in the presence of 0.5 μ M (A), 10 μ M (B), or 100 μ M (C) CuCl₂ in the culture media. Overlapping signal intensities were analyzed and quantitated by using FLUOVIEW FV500 Version 3.3 program. Each data point represents the mean \pm SEM from four separate experiments with a minimum of seven scans per experiment per data point. Each scan is comprised of 15–18 cells or at least 105 cells (*, $P < 0.001$ and #, $P < 0.05$ between *Atox1*^{+/+} and *Atox1*^{-/-} cells). Mean values were calculated, and differences were compared by using a one-way ANOVA with a Student-Newman-Keuls multiple comparison test.

sistent with previous findings in Chinese hamster ovary cells, revealing that during the course of such experiments some ATPase will be recycling to the Golgi compartment (4). Although some experimental variation was observed in these studies in the absolute percentage of Menkes ATPase trafficking out of the Golgi compartment (Fig. 3B 41% vs. Fig. 4A 59%), in each case a statistically significant quantitative difference was observed between BCS-treated *Atox1*^{+/+} and *Atox1*^{-/-} cells after copper supplementation.

Discussion

The data in this study indicate that Atox1 plays an essential role in the copper-mediated trafficking of the Menkes ATPase within

the secretory pathway. Previous studies have demonstrated that an increase in the intracellular copper content induces trafficking of the Wilson and Menkes copper-transporting P-type ATPases from the Golgi to a cytoplasmic vesicular compartment (4, 5). Detailed cell biological studies have revealed that copper stimulates the exocytic movement of these ATPases along the secretory pathway (6). The markedly decreased response of copper-mediated trafficking of the Menkes ATPase in *Atox1*-deficient cells after reduction of the intracellular copper content to that observed in wild-type cells (Fig. 4A and Table 1) indicates that, under physiologic conditions, such trafficking is mediated by means of Atox1. These findings are not the result of adaptation of the *Atox1*^{-/-} cells to increased copper, because the copper content of wild-type and *Atox1*-deficient cells under these experimental conditions was identical (Table 1) and over-expression of Atox1 in the deficient cells restores this responsiveness to increased copper (data not shown). Although the precise mechanisms underlying this response remain to be elucidated, recent studies have revealed a direct relationship between ATPase catalytic activity and copper-mediated trafficking, suggesting that copper transfer by Atox1 may play a critical role in this activation process (20).

In addition to revealing a critical role for Atox1 in copper-mediated ATPase trafficking, the results shown here also indicate that this requirement can be overcome under conditions where the intracellular copper content is increased (Fig. 4C). This finding is consistent with the observation that, in *Atox1*^{-/-} cells grown under basal conditions, the Menkes ATPase is localized predominantly in the cytoplasmic compartment in accord with the impaired copper efflux and elevated intracellular copper content found in these cells (Fig. 1B and Table 1) (14). The observation that the requirement for Atox1 in copper-mediated ATPase trafficking can be overcome with excess copper is analogous to studies in *Saccharomyces cerevisiae*, demonstrating that the requirement for each of the known copper chaperones can be at least partially obviated by growth of chaperone-deficient yeast in media with excess copper (7, 21, 22). A similar finding has been recently reported in mammalian cells, where copper supplementation of the media has been shown to restore cytochrome oxidase activity in cells derived from individuals with defects in the mitochondrial copper chaperone SCO2 (23, 24).

Importantly, the total intracellular copper content is identical in *Atox1*^{+/+} and *Atox1*^{-/-} cells at each copper supplemented concentration after BCS treatment (Table 1). This finding is in contrast to that observed in cells grown in basal media and reflects the hierarchy of copper trafficking to intracellular compartments in the first few hours of supplementation after copper depletion. Significant movement of copper to the secretory pathway and subsequent copper efflux is only restored once other intracellular compartments are replenished (2). Consistent with this concept, metabolic studies with ⁶⁴Cu revealed minimal copper efflux in *Atox1*^{+/+} and *Atox1*^{-/-} cells during this early phase of copper supplementation (data not shown). Indeed, it is this aspect of intracellular copper homeostasis that provides the experimental situation allowing Menkes ATPase localization to be examined in both cell types under equivalent intracellular copper content. Beyond these early time points, as cellular copper homeostasis is restored, the impairment in copper efflux in *Atox1*^{-/-} cells (14) eventually results in a significant increase in intracellular copper content in these cells compared with that observed in *Atox1*^{+/+} cells in the same media (Fig. 1B). The quantitative assessment in this current study reveals a marked decrease in the trafficking of the Menkes ATPase in the absence of Atox1 during this early period, supporting the concept that this chaperone plays a critical role in copper-mediated ATPase trafficking and, at steady state, cellular copper efflux under the

physiological conditions of limited availability of free copper within the cell (7).

The findings reported here also reveal a second critical aspect of Atox1 function. Although an elevation in the intracellular copper content in *Atox1*^{-/-} cells under basal conditions results in movement of the Menkes ATPase from the Golgi compartment (Fig. 2B), copper homeostasis in these cells remains markedly impaired as revealed by copper retention (Fig. 1B) and efflux studies (14). These data may be explained either by a critical requirement for Atox1 in the precise trafficking and localization of the Menkes ATPase or in the subsequent function of this ATPase in copper transport. The immunofluorescent data suggest that, under conditions of increased intracellular copper (100 μ M), the localization of the Menkes ATPase in the cytoplasmic vesicular compartment is identical in *Atox1*^{+/+} and *Atox1*^{-/-} cells (Fig. 3A). Although these observations mitigate the possibility that Atox1 deficiency alters the precise cytoplasmic vesicular localization of the copper-transport ATPases, further confirmation of this concept must await identification of additional markers that colocalize with these ATPases in this vesicular compartment. Support for the concept that Atox1 may be required directly for ATPase function comes from structural studies that reveal direct interaction of Atox1 with the copper-transport ATPases that depends on the copper-binding cysteine residues present in each of these proteins (25). These structural data provide a model for Atox1 in determining the specificity of ATPase copper transport that is further supported by kinetic studies indicating a direct role for Atox1 in copper-dependent ATPase phosphorylation (13). Consistent with such a role for Atox1 in ATPase function, the increase in Menkes

ATPase abundance observed in *Atox1*^{-/-} cells (Fig. 2A) was without effect on intracellular copper content, in contrast to previous observations in cells overexpressing the Menkes ATPase, where sufficient Atox1 was present (4). Regardless of the precise mechanism, the data reported here reveal an absolute requirement for Atox1 beyond the essential role in initiating copper-dependent trafficking of the ATPases from the Golgi compartment.

Taken together, the data in this study provide a cell biological model for the role of Atox1 under the physiological conditions of copper limitation in mammalian cells. This model permits a rationale physiologic explanation for the severity of the phenotype observed previously in *Atox1*^{-/-} mice that are born severely copper-deficient with a marked impairment in placental copper transfer despite elevated placental copper content (14). The recognition that Atox1 is essential for the copper-mediated trafficking of the Menkes ATPase provides further mechanistic insights into this critical posttranslational process of intracellular copper homeostasis. These findings may also now direct future studies into the role of additional components required for copper trafficking in the secretory pathway, including murr1, a novel cytoplasmic protein, recently identified as a candidate in Bedlington copper toxicosis (26).

We thank Mick Petris for sharing information before publication and helpful discussions, Betty Eipper and David Williams for sharing of reagents, Brian Bennett for guidance with confocal microscopy, and Louis Muglia and Guojun Bu for critical review of the manuscript. This work was supported by National Institutes of Health Grants DK61763 (to J.D.G.) and DK51899 (to I.H.).

1. Pena, M. M., Lee, J. & Thiele, D. J. (1999) *J. Nutr.* **129**, 1251–1260.
2. Culotta, V. C. & Gitlin, J. D. (2001) in *The Metabolic and Molecular Bases of Inherited Diseases*, eds. Scriver, C. R., Beaudet, A. L., Sly, W. S. & Valle, D. (McGraw-Hill, New York), Vol. 2, pp. 3105–3126.
3. Llanos, R. M. & Mercer, J. F. (2002) *DNA Cell Biol.* **21**, 259–270.
4. Petris, M. J., Mercer, J. F., Culvenor, J. G., Lockhart, P., Gleeson, P. A. & Camakaris, J. (1996) *EMBO J.* **15**, 6084–6095.
5. Hung, I. H., Suzuki, M., Yamaguchi, Y., Yuan, D. S., Klausner, R. D. & Gitlin, J. D. (1997) *J. Biol. Chem.* **272**, 21461–21466.
6. Petris, M. J. & Mercer, J. F. (1999) *Hum. Mol. Genet.* **8**, 2107–2115.
7. Rae, T. D., Schmidt, P. J., Pufahl, R. A., Culotta, V. C. & O'Halloran, T. V. (1999) *Science* **284**, 805–808.
8. O'Halloran, T. V. & Culotta, V. C. (2000) *J. Biol. Chem.* **275**, 25057–25060.
9. Rosenzweig, A. C. (2001) *Acc. Chem. Res.* **34**, 119–128.
10. Huffman, D. L. & O'Halloran, T. V. (2001) *Annu. Rev. Biochem.* **70**, 677–701.
11. Hamza, I., Schaefer, M., Klomp, L. W. & Gitlin, J. D. (1999) *Proc. Natl. Acad. Sci. USA* **96**, 13363–13368.
12. Larin, D., Mekios, C., Das, K., Ross, B., Yang, A. S. & Gilliam, T. C. (1999) *J. Biol. Chem.* **274**, 28497–28504.
13. Walker, J. M., Tsivkovskii, R. & Lutsenko, S. (2002) *J. Biol. Chem.* **277**, 27953–27959.
14. Hamza, I., Faisst, A., Prohaska, J., Chen, J., Gruss, P. & Gitlin, J. D. (2001) *Proc. Natl. Acad. Sci. USA* **98**, 6848–6852.
15. Spector, D. L., Goldman, R. D. & Leinwand, L. A. (1998) *Cells: A Laboratory Manual* (Cold Spring Harbor Lab. Press, Plainview, NY).
16. Kelly, E. J. & Palmiter, R. D. (1996) *Nat. Genet.* **13**, 219–222.
17. Williams, D. A., Rosenblatt, M. F., Beier, D. R. & Cone, R. D. (1988) *Mol. Cell. Biol.* **8**, 3864–3871.
18. Prohaska, J. R. & Bailey, W. R. (1994) *J. Neurochem.* **63**, 1551–1557.
19. Subramaniam, V. N., Loh, E. & Hong, W. (1997) *J. Biol. Chem.* **272**, 25441–25444.
20. Petris, M. J., Voskoboinik, I., Cater, M., Smith, K., Kim, B. E., Llanos, R. M., Strausak, D., Camakaris, J. & Mercer, J. F. (2002) *J. Biol. Chem.* **277**, 46736–46742.
21. Glerum, D. M., Shtanko, A. & Tzagoloff, A. (1996) *J. Biol. Chem.* **271**, 14504–14509.
22. Lin, S. J., Pufahl, R. A., Dancis, A., O'Halloran, T. V. & Culotta, V. C. (1997) *J. Biol. Chem.* **272**, 9215–9220.
23. Jaksch, M., Paret, C., Stucka, R., Horn, N., Muller-Hocker, J., Horvath, R., Trepsch, N., Stecker, G., Freisinger, P., Thirion, C., et al. (2001) *Hum. Mol. Genet.* **10**, 3025–3035.
24. Salvati, L., Hernandez-Rosa, E., Walker, W. F., Sacconi, S., DiMauro, S., Schon, E. A. & Davidson, M. M. (2002) *Biochem. J.* **363**, 321–327.
25. Wernimont, A. K., Huffman, D. L., Lamb, A. L., O'Halloran, T. V. & Rosenzweig, A. C. (2000) *Nat. Struct. Biol.* **7**, 766–771.
26. van De Sluis, B., Rothuizen, J., Pearson, P. L., van Oost, B. A. & Wijnga, C. (2002) *Hum. Mol. Genet.* **11**, 165–173.